Roles of helix H69 of 23S rRNA in translation initiation

Qi Liu and Kurt Fredrick[1]

Ohio State Biochemistry Program, Department of Microbiology, and Center for RNA Biology, The Ohio State University, Columbus, OH 43210

Edited by Harry F. Noller, University of California, Santa Cruz, CA, and approved August 7, 2015 (received for review April 20, 2015)

Initiation of translation involves the assembly of a ribosome complex with initiator tRNA bound to the peptidyl site and paired to the start codon of the mRNA. In bacteria, this process is kinetically controlled by three initiation factors—IF1, IF2, and IF3. Here, we show that deletion of helix H69 (ΔH69) of 23S rRNA allows rapid 50S docking without concomitant IF3 release and virtually eliminates the dependence of subunit joining on start codon identity. Despite this, overall accuracy of start codon selection, based on rates of formation of elongation-competent 70S ribosomes, is largely uncompromised in the absence of H69. Thus, the fidelity function of IF3 stems primarily from its interplay with initiator tRNA rather than its anti-subunit association activity. While retaining fidelity, ΔH69 ribosomes exhibit much slower rates of overall initiation, due to the delay in IF3 release and impedance of an IF3-independent step, presumably initiator tRNA positioning. These findings clarify the roles of H69 and IF3 in the mechanism of translation initiation and explain the dominant lethal phenotype of the ΔH69 mutation.

ribosome | IF2 | IF3 | fMet-tRNA | start codon selection

Translation initiation can be divided into two major stages in bacteria. The first stage involves assembly of the 30S initiation complex (30SIC). Facilitated by three initiation factors, initiator tRNA (*N*-formyl-methionyl-tRNA^{fMet}, or fMet-tRNA^{fMet}) binds to the peptidyl (P) site of the 30S subunit and pairs with the start codon on the mRNA. During the second stage, the 50S subunit associates with the 30SIC and triggers dissociation of the initiation factors, leaving the 70S initiation complex (70SIC) with fMet-tRNA^{fMet} in the P site, ready for elongation. Because initiation is the rate-limiting step of translation and establishes the reading frame, efficient and accurate assembly of the 70SIC is critical for cell survival.

30SIC assembly can be considered a largely random-order process, although there is a preferred kinetic pathway of ligand binding. IF2 and IF3 are generally first to bind to the 30S subunit, followed by IF1 and fMet-tRNA^{fMet}, whereas the timing of mRNA binding depends on its sequence context and cellular concentration (1). The three initiation factors reciprocally stabilize one another in the 30SIC, and their binding induces a conformational change of the subunit, including a clockwise rotation of the head domain (2). IF1 is an 8-kDa protein that binds to helix h44, the 530 loop, and the S12 region and blocks the 30S aminoacyl (A) site (3). IF2 is a multidomain ribosome-dependent GTPase that makes extensive contacts with both the 30S subunit and fMet-tRNA^{fMet}. Domains G3 and C1 of IF2 bind helix h5 and h14 of 16S rRNA, the N-terminal domain (NTD) interacts with S16 and IF1, and domain C2 recognizes the acceptor stem and fMet moiety of fMet-tRNA^{fMet} (2, 4). These interactions contribute to functions of IF2 in increasing the on rate of fMet-tRNA^{fMet} binding and discriminating against elongator tRNAs (5). IF3 consists of two globular domains connected by a flexible linker (6, 7). Based on structural studies of the 30SIC, the C-terminal domain (CTD) binds to the 30S platform near helices h23, h24, and h45 of 16S rRNA (8), whereas the NTD of IF3 has been modeled to interact with the elbow region of fMet-tRNA^{fMet} (2). The presence of IF3 in the 30SIC induces a conformational change of IF2 and fMet-tRNA^{fMet} (2, 9) and increases both on and off rates of tRNA binding (5). IF1 enhances the effects of IF2 and IF3 on tRNA stability (5). Together, all three initiation factors tune the kinetics of fMet-tRNA^{fMet} binding for optimal efficiency and fidelity.

Formation of 70SIC is highly dependent on fMet-tRNA^{fMet} and IF2 (10), which together provide a large surface area complementary to the 50S interface (11, 12). 50S docking stimulates the GTPase activity of IF2 (13), presumably through the interaction between the sarcin–ricin loop and IF2 G domain, and triggers a large conformational change that favors factor dissociation (12). This is accompanied by movement of the initiator tRNA into the P/P site (14). IF3 inhibits subunit joining, an effect more pronounced in the presence of noncanonical codon–anticodon base pairing (5, 15). The mechanism by which IF3 prevents spurious initiation likely involves its interplay with fMet-tRNA^{fMet}. IF3 and tRNA are mutually destabilizing; thus, noncanonical base pairing delays IF3 dissociation and 70SIC formation (10, 16, 17). More recently, it was shown that the conformation of IF3 in the 30SIC is also sensitive to the identity of the start codon (18).

Helix H69 of 23S rRNA is a highly conserved element located at the 50S interface and interacts extensively with helix h44 of 16S rRNA through intersubunit bridge B2a (Fig. 1) (19). In the elongation complex, H69 also makes direct contact with P-site tRNA at nucleotides 11–13 and 24–25 in the D stem-loop region (20). Deletion of H69 (ΔH69, Fig. 1*C*) has been shown to cause dominant lethality in vivo and a severe subunit association defect in vitro that can only be partially rescued in the presence of mRNA, tRNA, and a high concentration of Mg^{2+} (21). Despite these strong effects, ΔH69 ribosomes are fully competent for in vitro poly-Phe synthesis (21) and are only mildly affected in translocation (22). During subunit association, bridge B2a is among the earliest interactions formed between the two subunits (23), and H69 is in close proximity to the binding sites of initiator tRNA and IF3 (11, 12). Thus, the interplay between H69 and these ligands may be central to the molecular mechanism of 70SIC formation.

In the current study, we investigate the effects of H69 deletion on 70SIC formation. We find that the ability of IF3 to regulate 50S docking depends largely on H69. Loss of H69 delays the release of IF3 and inhibits a subsequent conformational change of fMet-tRNA^{fMet} that leads to formation of elongation-competent 70SIC. Our data support a model in which H69 is critical for coupling IF3 dissociation with subunit joining as well as regulating

Significance

In this work, we dissect the interplay between helix H69 of the large subunit ribosomal RNA, initiation factor IF3, and initiator tRNA, interactions upon which the speed and accuracy of translation initiation rely. Our data clarify the molecular mechanisms that control the initiation process and explain the essentiality of H69 in the cell.

Author contributions: Q.L. and K.F. designed research; Q.L. performed research; Q.L. and K.F. analyzed data; and Q.L. and K.F. wrote the paper.

The authors declare no conflict of interest.

This article is a PNAS Direct Submission.

[1]To whom correspondence should be addressed. Email: fredrick.5@osu.edu.

This article contains supporting information online at www.pnas.org/lookup/suppl/doi:10.1073/pnas.1507703112/-/DCSupplemental.

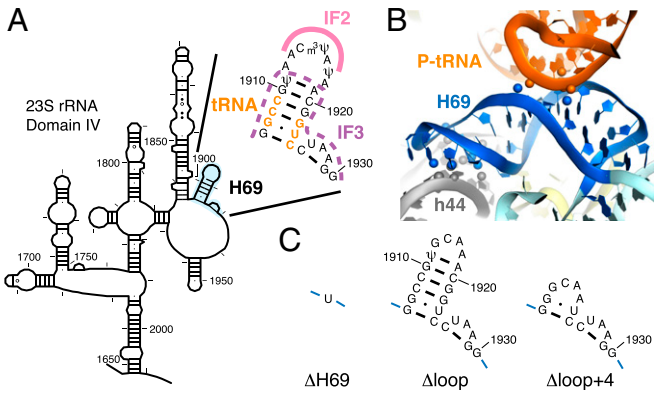

Fig. 1. Location and structure of H69 in the ribosome. (*A*) Secondary structure of H69 and its location in the 23S rRNA [schematic diagram adapted from the Comparative RNA Website (35)]. Nucleotides making contact with P-site tRNA are highlighted in orange, regions predicted to interact with IF2 are marked with a pink line, and regions predicted to clash with IF3 are indicated by a dashed purple line. (*B*) Tertiary structure of H69 in the 70S ribosome [based on Protein Data Bank ID codes 2WDG and 2WDI (20)]. Atoms involved in interactions between H69 and P-site tRNA or helix h44 of 16S rRNA are shown in spheres. (*C*) Nucleotides replacing the native sequence (nt 1906–1930) in ΔH69, ΔLoop, and ΔLoop+4 mutants.

fMet-tRNA^{fMet} movement during the second stage of translation initiation.

Results

H69 Is Important for Start Codon Selection During 50S Docking. To study the function of H69 in subunit joining in vitro, control (WT) and mutant (ΔH69) 50S subunits were purified, and the apparent rates of 50S docking to preassembled 30SIC, with either a cognate AUG or near-cognate AUC start codon, were measured using stopped-flow spectrometry. Mixing WT 50S subunits with 30SIC(AUG) resulted in a biphasic increase in light scattering (LS), with fast (2.0 s^{-1}) and slow (0.28 s^{-1}) phases accounting for ~60% and ~40% of the total amplitude (Fig. 2*A*, Fig. S1, and Table 1). Biphasic increases in LS have been reported in earlier studies and were attributed to either two-step 50S docking (14) or functional heterogeneity of the 30SIC, in which a fraction of the 30S complexes exist in a docking-incompetent state at the time of mixing (16, 24). The latter may be more pertinent to the current study, as our data most closely resemble those of Rodnina and coworkers (16). In our hands, k_{app1} and k_{app2} increase with 50S concentration in the range tested (0.1–0.4 μM), giving an association rate constant for the fast phase of 15 $\mu M^{-1}{\cdot}s^{-1}$ (Fig. S2), results quite similar to those reported by Milon et al. (16). The somewhat slower association kinetics seen here, compared with previous work (25), stems from the use of affinity-purified 50S subunits. When the start codon was replaced with AUC, the apparent rate of 50S docking decreased by >30-fold for both fast (0.064 s^{-1}) and slow (0.0064 s^{-1}) phases, in agreement with previous reports (16, 25).

Deletion of H69 had subtle effects on 50S docking to 30SIC (AUG), slightly increasing k_{app1} and A_1, while slightly decreasing k_{app2} and A_2 (Fig. 2*A* and Table 2). In the presence of AUC, however, ΔH69 strongly stimulated 50S docking. For ΔH69 50S, k_{app1} and k_{app2} were 37-fold and 17-fold faster than those of WT 50S, whereas A_1 and A_2 were almost unchanged. The apparent rates of ΔH69 50S docking were essentially indistinguishable between 30SIC(AUG) and 30SIC(AUC), indicating that H69 is important for controlling subunit joining in response to the start codon. The decreased amplitude of LS change in near-cognate complexes indicates that less 70SIC is formed in the presence of AUC. This is likely due to weaker binding of fMet-tRNA^{fMet} in 30SIC(AUC), compared with 30SIC(AUG) (16, 17). In line with this idea, little LS change was observed in the absence of fMet-tRNA^{fMet} for both WT and ΔH69 ribosomes (Fig. 2*A*), indicating that LS change is largely dependent on fMet-tRNA^{fMet}.

H69 Is Critical for IF3 Regulation of 50S Docking. IF3 is well known as an "antiassociation" factor that negatively regulates translation initiation to enhance start codon selection (26). In line with previous reports (10, 15, 16), omission of IF3 from 30SIC stimulated subunit joining in WT ribosomes, an effect most prominent in the presence of AUC (Fig. 2*B* and Table 1). For 30SIC(AUC), removal of IF3 increased k_{app1} and k_{app2} by 47-fold and 17-fold, respectively, to values nearly as high as those seen with 30SIC(AUG). These data suggest that the difference in WT 50S docking to cognate and near-cognate 30SICs is dependent on IF3. In contrast, docking of ΔH69 50S was largely unaffected by IF3, regardless of whether AUG or AUC was present. These data indicate that loss of H69 compromises the ability of IF3 to regulate 50S docking in response to different start codons. A higher concentration of IF3 can inhibit 50S docking in both WT and ΔH69 ribosomes, evident from slower apparent rates and smaller amplitudes in LS change (Fig. 2*C* and Fig. S3). The apparent rate of 50S docking has a reciprocal dependence on the concentration of IF3, consistent with earlier evidence that stable 70SIC formation requires IF3 release (10). The IC_{50} of IF3 for ΔH69 50S is about fivefold higher than that of WT 50S; hence, the inhibitory function of IF3 in subunit joining is clearly compromised in the absence of H69. Because IF3 and fMet-tRNA^{fMet} are known to destabilize each other in the 30SIC (5, 16), inhibition of ΔH69 50S docking at high concentrations of IF3 may be due to a strong leftward equilibrium shift of the 30SIC assembly pathway under these conditions.

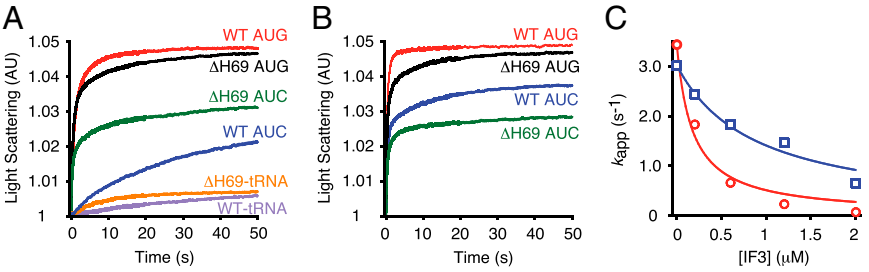

Fig. 2. H69 is important for IF3 regulation of subunit joining. (*A* and *B*) Apparent rates of 50S docking were measured by mixing preassembled 30SIC with WT (AUC, blue; AUG, red) or ΔH69 (AUC, green; AUG, black) 50S subunits, in the presence (*A*) or absence (*B*) of IF3. Data were fit to a double-exponential equation to obtain apparent rates shown in Table 1. AU, arbitrary units. (*C*) Apparent rates of 50S docking were plotted against IF3 concentration for WT (red circles) and ΔH69 (blue squares) ribosomes. Data were fitted to the modified dose–response equation $k_{app} = k_{max}/[1 + (IF3)/IC_{50}]$ to obtain IC_{50} values. WT, IC_{50} = 0.17 μM; ΔH69, IC_{50} = 0.87 μM.

Table 1. Apparent rates of 50S docking

50S	30S complex	Start Codon	k_{app1}, s^{-1}	A_1	k_{app2}, s^{-1}	A_2
WT	30SIC	AUG	2.0 ± 0.4	0.033 ± 0.010	0.28 ± 0.03	0.019 ± 0.001
		AUC	0.064 ± 0.014	0.016 ± 0.001	0.0064 ± 0.0008	0.021 ± 0.005
	30SIC-IF3	AUG	3.4 ± 0.1	0.039 ± 0.001	0.64 ± 0.01	0.0087 ± 0.0001
		AUC	2.8 ± 0.1	0.024 ± 0.001	0.11 ± 0.05	0.011 ± 0.001
ΔH69	30SIC	AUG	2.4 ± 0.5	0.037 ± 0.009	0.16 ± 0.04	0.013 ± 0.002
		AUC	2.4 ± 0.4	0.017 ± 0.004	0.11 ± 0.02	0.013 ± 0.002
	30SIC-IF3	AUG	3.0 ± 0.1	0.031 ± 0.001	0.17 ± 0.02	0.011 ± 0.001
		AUC	2.7 ± 0.1	0.020 ± 0.001	0.21 ± 0.02	0.0064 ± 0.0001
ΔLoop	30SIC	AUG	1.7 ± 0.5	0.020 ± 0.005	0.39 ± 0.14	0.017 ± 0.003
		AUC	0.11 ± 0.02	0.0039 ± 0.0009	0.021 ± 0.003	0.0046 ± 0.0006
ΔLoop+4	30SIC	AUG	2.3 ± 0.3	0.030 ± 0.003	0.45 ± 0.11	0.011 ± 0.001
		AUC	0.18 ± 0.06	0.0067 ± 0.0018	0.015 ± 0.004	0.0054 ± 0.0010

At least three independent experiments were performed to generate the parameters shown in all tables (mean ± SD). Each independent experiment entailed four or more replicas of rapid mixing (shots).

H69 Promotes IF3 Dissociation During Initiation. Chemical probing and cryo-EM studies suggest that the position of IF3 CTD in the 30SIC overlaps with that of H69 in the context of the 70S ribosome, raising the hypothesis that competition between H69 and IF3 for 30S binding is key to the mechanism of IF3 (2, 8). Deletion of H69 may remove the steric clash between IF3 and 50S and hence allow subunit joining without IF3 dissociation. To test this idea, we monitored IF3 dissociation during formation of WT or ΔH69 70SIC using Förster Resonance Energy Transfer (FRET). Alexa Fluor 555 was introduced at position 135 of IF3, where modifications were previously shown to have no detrimental effects on factor function (8). DyLight 647 was incorporated on to 30S subunit protein S7 engineered with a C-terminal Sfp tag (27) (30S-DY647) and was used as a fluorescence acceptor in combination with IF3-AF555 (IF3-30S FRET). The Spf tag was designed to replace the nonconserved extension of S7 characteristic of *Escherichia coli K* strains (28), and the engineered *rpsG*-Spf strain, containing only this tagged version of the S7 gene, grew as rapidly as the WT control strain. Both IF3-AF555 and 30S-DY647 were completely functional in 70SIC formation, based on the comparable rates with which dual-labeled and unlabeled complexes assemble and form the first peptide bond (Fig. S4). Steady-state fluorescence spectra showed that the presence of both IF3-AF555 and 30S-DY647 in the 30SIC results in a clear FRET signal, with an estimated efficiency of 0.28 (Fig. S5*A*). Addition of excess unlabeled IF3 to the dual-labeled 30SIC virtually eliminated FRET, consistent with dissociation of IF3-AF555 from 30S-DY647.

Upon mixing with WT 50S subunits, 30SIC preassembled with both donor and acceptor fluorophores (D+A) showed a rapid decrease in acceptor fluorescence (Fig. S5*B*). Control experiments with only acceptor (A) or donor (D) present showed little fluorescence change, indicating that the observed fluorescence change in the D+A case is due to the decrease in FRET efficiency. The decrease in IF3-30S FRET upon 50S docking was biphasic (Fig. 3*A*, Fig. S6, and Table 2), with k_{app1} (1.7 s^{-1}) and k_{app2} (0.18 s^{-1}) closely resembling those of the LS measurement (Table 1). When the start codon was replaced with AUC, the apparent rates of FRET change decreased by >25-fold for both fast (0.068 s^{-1}) and slow (0.0051 s^{-1}) phases. Mixing dual-labeled 30SIC with excess unlabeled IF3 resulted in notably faster decreases of acceptor fluorescence than those seen with 50S subunits, whereas rates remained highly responsive (>30-fold) to the start codon sequence (Fig. S5*C*). These data are in line with earlier reports (16) and provide evidence that the observed FRET changes are related to IF3 dissociation. Furthermore, they suggest that the apparent rate of IF3 dissociation in the initiation reaction reflects that of subunit joining, which at least under these conditions is smaller than the intrinsic dissociation rate (k_{off}) of IF3 from the 30SIC.

When ΔH69 50S subunits were mixed with 30SIC(AUG), the amplitude of the rapid IF3-30S FRET change, A_1, was reduced substantially (2.4-fold), whereas A_2 was increased by 60% (Fig. 3*A* and Table 2). These data suggest a lag in the release of IF3, despite that 50S docking is largely unaffected (Fig. 2*A* and Table 1). A similar effect of ΔH69 was seen in the presence of AUC, where A_1 and A_2 were reduced threefold and 2.2-fold, respectively,

Table 2. Apparent rates of FRET changes related to IF3 dissociation during 70SIC formation

FRET pair	50S	Start codon	k_{app1}, s^{-1}	A_1	k_{app2}, s^{-1}	A_2
IF3-30S	WT	AUG	1.7 ± 0.1	0.085 ± 0.002	0.18 ± 0.01	0.036 ± 0.003
		AUC	0.068 ± 0.006	0.069 ± 0.006	0.0051 ± 0.0001	0.14 ± 0.01
	ΔH69	AUG	2.9 ± 0.1	0.036 ± 0.002	0.043 ± 0.004	0.057 ± 0.002
		AUC	0.070 ± 0.003	0.023 ± 0.003	0.0079 ± 0.0004	0.064 ± 0.001
	ΔLoop	AUG	1.5 ± 0.2	0.084 ± 0.002	0.26 ± 0.02	0.027 ± 0.002
	ΔLoop+4	AUG	2.6 ± 0.3	0.10 ± 0.01	0.29 ± 0.01	0.019 ± 0.002
tRNA-IF3	WT	AUG	1.9 ± 0.4	0.022 ± 0.002	0.11 ± 0.01	0.032 ± 0.002
		AUC	0.035 ± 0.004	0.017 ± 0.001	0.0018 ± 0.0004	0.036 ± 0.013
	ΔH69	AUG	0.041 ± 0.003	0.016 ± 0.003	0.0017 ± 0.0003	0.039 ± 0.014
		AUC*	0.22 ± 0.03	−0.0071 ± 0.0005	0.0015 ± 0.0002	0.018 ± 0.010
	ΔLoop	AUG	1.5 ± 0.1	0.028 ± 0.002	0.22 ± 0.03	0.012 ± 0.002
	ΔLoop+4	AUG	2.3 ± 0.2	0.043 ± 0.002	0.22 ± 0.04	0.015 ± 0.004

*When mixing 30SIC(AUC) and H69 50S, there is a fast phase of tRNA-IF3 FRET increase (denoted as a negative A_1) and a slow phase of FRET decrease (*Results* and Fig. 2).

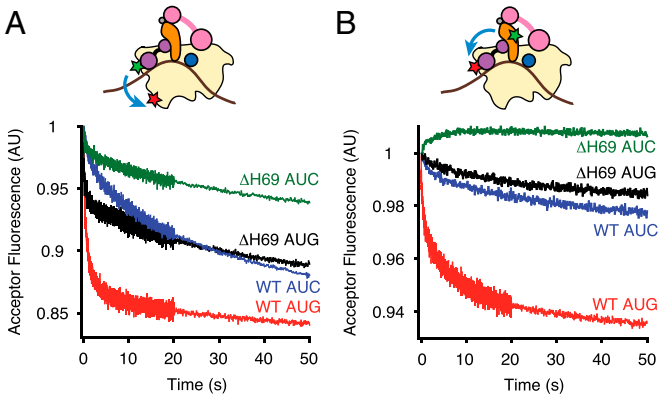

Fig. 3. Dissociation of IF3 during initiation depends on H69. Apparent rates of (*A*) IF3-30S or (*B*) tRNA-IF3 FRET changes were measured by mixing preassembled 30SIC with WT (AUC, blue; AUG, red) or ΔH69 (AUC, green; AUG, black) 50S subunits. Data were fit to a double-exponential equation to obtain apparent rates shown in Table 2. 30S, pale yellow; acceptor fluorophore, red star; donor fluorophore, green star; fMet-tRNA^{fMet}, orange; IF1, dark blue; IF2, pink; IF3, purple; mRNA, brown.

relative to the WT 50S case (Fig. 3*A* and Table 2). These data suggest that, in the absence of H69, a substantial fraction of IF3 fails to dissociate upon or after 50S docking.

To analyze IF3 dissociation from another perspective, we used IF3-AF555 as a fluorescence acceptor in conjunction with Oregon Green 488 attached to 4-thiouridine at position 8 of fMet-tRNA^{fMet} (tRNA-OG488). tRNA^{fMet} modified in this manner has been shown to be functional in initiation (1, 9, 16, 29, 30). Because fMet-tRNA^{fMet} remains in the ribosomal P site during subunit joining, we reasoned that IF3 release during initiation would cause a decrease in the tRNA-IF3 FRET signal. Although 30SICs containing these fluorophores exhibited a rather low FRET efficiency (0.14; Fig. S7*A*), stopped-flow experiments showed a clear decrease in acceptor fluorescence upon mixing with excess unlabeled IF3 or 50S subunits that depends on both donor and acceptor dyes (Fig. S7 *B* and *C*), consistent with loss of FRET due to IF3 dissociation. This FRET decrease also exhibited biphasic kinetics (Fig. 3*B* and Fig. S8), with apparent rates for the WT ribosome matching fairly well with those of the LS and IF3-30S FRET experiments described above, in both the AUG and AUC cases (Table 2).

When ΔH69 50S subunits were mixed with 30SIC(AUG), the tRNA-IF3 FRET decreased slowly, with k_{app1} and k_{app2} 46-fold and 65-fold smaller than in the WT case. These data are generally consistent with the IF3-30S FRET data, in that both experiments suggest a delay in IF3 release. However, the fact that ΔH69 primarily reduces amplitudes in the former case and reduces rates in the latter is puzzling and incongruent with the idea that all observed FRET decreases reflect IF3 release. A possible explanation is that, in the absence of H69, k_{app2} of IF3-30S FRET (0.043 ± 0.004 s^{-1}) and k_{app1} of tRNA-IF3 FRET (0.041 ± 0.003 s^{-1}) report on the same event—IF3 dissociation—and k_{app1} of IF3-30S FRET corresponds to a preceding conformational change in the ligand bound complex (e.g., movement of residue 135 of IF3 away from the C terminus of S7) (Table 2). Consistent with this idea, formation of elongation-competent 70SIC(ΔH69), which presumably requires factor dissociation, is somewhat slower (0.018 s^{-1}; Table 3; see *H69 Is Needed for the Formation of Elongation-Competent 70SIC*) than k_{app2} of IF3-30S FRET. When ΔH69 50S subunits were mixed with 30SIC(AUC), the tRNA-IF3 FRET signal increased slightly and then decreased very slowly (Fig. 3*B*). The initial increase (0.22 s^{-1}) presumably corresponds to a conformational change, whereas the slow decrease may (at least in part) reflect retarded IF3 release. Notably, the net amplitude for this reaction was a small decrease in FRET that amounted to ∼20% of that seen in the presence of H69 (Table 2). This suggests that a large fraction of the IF3 remains bound after ΔH69 50S docking, corroborating the conclusion drawn above from the IF3-30S FRET data.

H69 Is Needed for the Formation of Elongation-Competent 70SIC. Because dissociation of initiation factors is important for mature 70SIC formation, we hypothesized that ΔH69 may slow later steps in the initiation process. To test this idea, we measured the rate at which 70SIC becomes reactive for dipeptide formation under single-turnover conditions, in the presence or absence of IF3, using rapid quench flow. Preassembled 30SIC was mixed with an excess of control or mutant 50S subunits and the ternary complex for codon 2 of the mRNA, and the amount of dipeptide formed was quantified as a function of time (Fig. 4*A*). For WT 50S subunits, the apparent rate for 30SIC(AUG) and 30SIC (AUC) was 0.34 s^{-1} and 0.017 s^{-1}, respectively (Table 3), representing ∼20-fold discrimination against AUC. When IF3 was omitted from the WT ribosomes, k_{app} increased by twofold and 36-fold in the presence of AUG and AUC, respectively, and the difference between cognate and near-cognate complexes was almost eliminated, corroborating the importance of IF3 in translation fidelity. For ΔH69 50S subunits, apparent rates of dipeptide formation were much slower than the WT, for both 30SIC(AUG) (∼20-fold) and 30SIC(AUC) (∼sixfold), whereas the fidelity was mostly retained ($k_{app,\ AUG}/k_{app,\ AUC}$ = 7.2). Omission of IF3 from ΔH69 ribosomes resulted in an 11-fold and 64-fold increase in k_{app} in the presence of AUG and AUC, respectively, an effect more pronounced than that seen for the WT. In the absence of IF3, ΔH69 ribosomes exhibited no discrimination against AUC but were still slower in dipeptide formation than the WT, indicating that the mutation also confers defects unrelated to IF3 function.

To verify that the inhibitory effect of ΔH69 on dipeptide formation is due to a defect in initiation rather than peptide bond formation, we repeated the experiments with nonenzymatically assembled 70S complexes (Table 3, 70S). Indeed, there was

Table 3. Apparent rates of dipeptide formation

Preassembled complex	Start codon	k_{app}, s^{-1}			
		WT	ΔH69	Δloop	Δloop+4
30SIC	AUG	0.34 ± 0.04	0.018 ± 0.003	0.087 ± 0.011	0.085 ± 0.02
	AUC	0.017 ± 0.005	0.0025 ± 0.0006	0.0077 ± 0.0033	0.0068 ± 0.0013
30SIC-IF3	AUG	0.82 ± 0.13	0.20 ± 0.02	0.14 ± 0.02	0.16 ± 0.02
	AUC	0.62 ± 0.26	0.16 ± 0.03	0.12 ± 0.01	0.10 ± 0.01
70SIC	AUG	2.0 ± 0.3	0.032 ± 0.006	0.14 ± 0.01	0.17 ± 0.05
70SIC-IF1	AUG	1.7 ± 0.3	0.038 ± 0.004	0.14 ± 0.01	0.16 ± 0.02
70SIC-IF3	AUG	1.9 ± 0.1	0.44 ± 0.14	0.19 ± 0.05	0.18 ± 0.03
70S	AUG	2.9 ± 0.6	1.8 ± 0.1	1.4 ± 0.3	1.3 ± 0.3

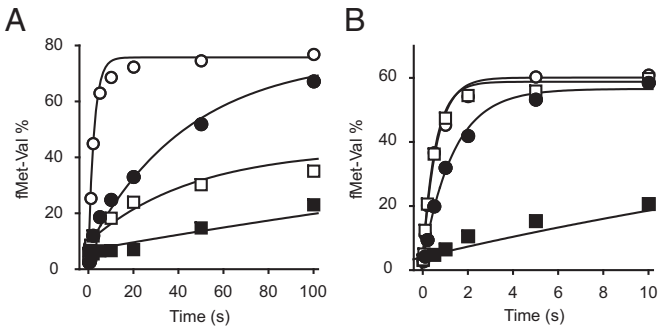

Fig. 4. Formation of elongation-competent 70SIC depends on H69. (*A*) Apparent rates of dipeptide formation were measured after mixing preassembled 30SIC with WT (open symbols) or ΔH69 (closed symbols) 50S subunits and ternary complex, in the presence of an AUG (circles) or AUC (squares) start codon. (*B*) Apparent rates of dipeptide formation were measured by mixing enzymatically preassembled WT (open symbols) or ΔH69 (closed symbols) 70SIC with ternary complex, in the presence (squares) or absence (circles) of IF3. Data were fit to a single-exponential equation to obtain apparent rates shown in Table 3.

virtually no difference in the apparent rate between WT (2.9 s^{-1}) and ΔH69 (1.8 s^{-1}) ribosomes. In parallel, when preassembled 70SIC was tested, the apparent rate of dipeptide formation in ΔH69 ribosomes (0.032 s^{-1}) was 62-fold slower than that of the WT (2.0 s^{-1}). These data show that the ΔH69 defect depends on initiation factors, consistent with a previous report (31), and suggest that ΔH69 traps the 70SIC in an intermediate conformation that cannot react with the ternary complex. Omission of IF1 from the 70SIC did not suppress this defect. However, omission of IF3 from the 70SIC increased k_{app} by 14-fold (Fig. 4*B* and Table 3). These data, together with the FRET experiments above, suggest that the defect of ΔH69 ribosomes in forming elongation-competent 70SIC is largely due to the inability of IF3 to dissociate from the complex in the absence of H69.

H69 Facilitates Steps of Initiation Independent of IF3. Omission of IF3 from the 70SIC did not restore the apparent rate of dipeptide formation in ΔH69 ribosomes to the value seen for the WT (Table 3). This suggests that, during 70SIC formation, factors other than IF3 are affected by deletion of H69. Previous cryo-EM studies indicate that fMet-tRNA^{fMet} in the 30SIC adopts a different conformation than the P/P tRNA in the 70S ribosome, with its elbow region tilted and acceptor stem shifted, changes presumably induced by interactions with IF2 and IF3 (2). During 70SIC formation, fMet-tRNA^{fMet} would need to undergo a conformational change to move its acceptor stem into the 50S P site for efficient dipeptide formation. In the crystal structure of the 70S elongation complex, the stem region of H69 (nucleotides 1907–1909 and 1922–1924) is in direct contact with the P-site tRNA (20). This raises the possibility that H69 is important for the proper alignment of fMet-tRNA^{fMet} during 70SIC formation, an activity independent of IF3. To test this, we constructed and purified 50S subunits with partial deletions of H69: ΔLoop, in which the loop region of H69 is replaced by a GCAA tetraloop, and ΔLoop+4, in which four additional base pairs are removed (Fig. 1*C*). Neither truncation is predicted to eliminate the steric clash between IF3 and the 50S subunit.

Both ΔLoop and ΔLoop+4 mutations had little to no effect on subunit joining in the presence of AUG (Table 1). When mixed with 30SIC(AUC), both ΔLoop and ΔLoop+4 50S subunits showed slight increases (2–3-fold) in k_{app1} and k_{app2} of 50S docking, compared with the WT. In contrast to ΔH69 ribosomes, but similar to the WT, both ΔLoop and ΔLoop+4 ribosomes were found to be capable of discriminating between AUG and AUC during subunit joining. When IF3 dissociation was measured using ΔLoop and ΔLoop+4 50S subunits, the kinetics were similar to those of WT ribosomes, for both IF3-30S and tRNA-IF3 FRET (Table 2). Together, these data suggest that the two partial deletions of H69 have little effect on the regulatory function of IF3 during 50S docking, or the coupling between IF3 dissociation and subunit joining. Hence, only complete removal of the steric clash between IF3 and the 50S subunit (i.e., ΔH69) can uncouple IF3 dissociation and subunit joining.

Both ΔLoop and ΔLoop+4 mutations showed a minor defect (~twofold) in peptide bond formation when 70S ribosomes were preassembled nonenzymatically (Table 3). In contrast, when 70SICs were formed in the presence of all initiation factors, apparent rates of dipeptide formation in ΔLoop and ΔLoop+4 ribosomes were much slower (12–14-fold) compared with the WT, an effect completely independent of IF1 or IF3. Similar defects were observed for both mutants when the reactions used preassembled 30SIC. Because partial deletion of H69 does not interfere with IF3 functions, the effects of ΔLoop and ΔLoop+4 on dipeptide formation suggest an additional IF3-independent role of H69 on fMet-tRNA^{fMet} positioning during 70SIC formation. Because ΔLoop and ΔLoop+4 were equally deleterious, this IF3-independent role can be attributed to the loop region of H69, which forms intersubunit bridge B2a.

Discussion

IF3 has a well-established role in preventing spurious initiation (15, 16, 32, 33), but the molecular basis of this activity has remained unclear. It has been proposed that mutually exclusive interactions between IF3 and H69 on the 30S subunit are key to the function of IF3 in initiation (2, 8). Here we provide direct evidence that removal of this steric clash prevents IF3 from regulating subunit joining and efficiently leaving the IC. Our data are in line with structural studies (2, 8) and demonstrate that H69 is indeed important for triggering IF3 dissociation during 70SIC formation. Because the interplay between IF3 and H69 is likely to occur only after initial 50S docking, our data support a kinetic model in which initial formation of a 70S complex precedes IF3 dissociation, consistent with several previous studies (14, 16, 30). In this model, fast subunit joining leads to the formation of an unstable 70SIC intermediate (Fig. S9, 70SICi), in which IF3 remains bound to the ribosome and the acceptor stem of fMet-tRNA^{fMet} is tilted away from the 50S P site. In WT ribosomes, due to competitive binding of H69 to the 30S platform, IF3 is released from the 70SICi shortly after 50S docking, and fMet-tRNA^{fMet} is properly aligned to the P/P site with the help of H69. In ΔH69 ribosomes, although subunit joining occurs at a rate comparable to the WT, both IF3 dissociation and fMet-tRNA^{fMet} alignment are inhibited. Thus, deletion of H69 traps the IC at the 70SICi stage and prevents the complex from entering the elongation phase. This provides a plausible explanation to the dominant lethal phenotype of H69 deletion in vivo (21), as ΔH69 50S subunits would trap ICs in a nonproductive form and prevent components from being accessed by WT 50S subunits.

Helix H69 contributes to the central intersubunit bridge B2a, loss of which shifts the 30S + 50S ⇌ 70S equilibrium strongly leftward (21). However, our LS experiments show that ΔH69 50S subunits are capable of docking to the 30SIC, with rate and amplitude comparable to the WT (Fig. 2 and Table 1). This difference can be explained by the presence of IF2 in the 30SIC, which provides considerable surface area for 50S docking in the absence of H69. Interestingly, in contrast to ΔH69, both ΔLoop and ΔLoop+4 mutations reduce the amplitudes of 50S docking, an effect more dramatic in the presence of AUC (Table 1). These partial deletions of H69, similar to ΔH69, are predicted to remove interactions at bridge B2a between the H69 loop region and helix h44 of 16S rRNA (Fig. 1). The full competency of ΔH69 50S in subunit joining can be explained by the inability of

IF3 to inhibit 50S docking in this mutant (Fig. 2), which effectively compensates for the loss of bridge interactions. In the presence of partial deletions, however, IF3 retains its ability to inhibit 50S docking, and bridge B2a, which normally promotes 70S formation, is missing. The loss of B2a without loss of IF3 antiassociation activity can explain the reduced amplitude observed. Our results underscore the importance of bridge B2a formation during subunit joining (23), which effectively drives the reaction of 70SIC formation forward in the presence of IF3.

Although ΔH69 eliminates the difference in docking rates between cognate and near-cognate 30SICs (Table 1 and Fig. 2*A*), the mutation has little effect on fidelity of the overall reaction (Table 3 and Fig. 4*A*). Discrimination against AUC in ΔH69 ribosomes is clearly dependent on IF3 and occurs at steps later than subunit joining. Our FRET experiments show that IF3 dissociation from ΔH69 ribosomes, although uncoupled from 50S docking, is influenced by the identity of the start codon (Table 2 and Fig. 3). Thus, the function of IF3 in maintaining initiation fidelity does not rely on its ability to regulate subunit joining but results from its binding stability, which is influenced by the identity of the start codon (ref. 16 and this study). In addition, IF3 may alter the conformation of fMet-tRNA^{fMet} in the 30SIC through interaction of its NTD in response to the start codon and may change the reaction pathway of fMet-tRNA^{fMet} alignment during 70SIC formation. In line with this idea, recent single-molecule FRET studies have shown that both IF2 and IF3 adopt different conformations in cognate and near-cognate 30SICs (9, 34). Our data suggest that IF3 inhibits the forward reaction of 70SIC formation whenever it is bound and hence can enhance start codon selection at both early and late stages of initiation.

Methods

Reagents were prepared as described in *SI Methods*. LS experiments were performed essentially as described (25), as detailed in *SI Methods*. Rates of FRET changes were determined under the same conditions as LS experiments, except that labeled components (IF3-AF555 and 30S-DY647 or tRNA-OG488) were used. For IF3-30S FRET, the excitation wavelength was 500 nm, and a 645-nm cutoff filter was placed in front of the fluorescence detector to measure acceptor fluorescence. For tRNA-IF3 FRET, the excitation wavelength was 460 nm, and a 590-nm cutoff filter was used. Rates of dipeptide formation were determined using a rapid quench-flow machine (KinTeK), as detailed in *SI Methods*.

ACKNOWLEDGMENTS. We thank C. Squires and S. Quan for *E. coli* strain SQZ10, P. Schultz for *E. coli* strain Δ*rpsG* (pCDSSara-S7), H. Noller for plasmid pET24b-IF3(C65A/E135C), and D. Qin and S. McClory for preliminary data and technical help. This work was supported by National Science Foundation Grant MCB 1243997 (to K.F.) and a Presidential Fellowship (to Q.L.) from The Ohio State University.

1. Milón P, Maracci C, Filonava L, Gualerzi CO, Rodnina MV (2012) Real-time assembly landscape of bacterial 30S translation initiation complex. *Nat Struct Mol Biol* 19(6):609–615.
2. Julián P, et al. (2011) The cryo-EM structure of a complete 30S translation initiation complex from Escherichia coli. *PLoS Biol* 9(7):e1001095.
3. Carter AP, et al. (2001) Crystal structure of an initiation factor bound to the 30S ribosomal subunit. *Science* 291(5503):498–501.
4. Simonetti A, et al. (2008) Structure of the 30S translation initiation complex. *Nature* 455(7211):416–420.
5. Antoun A, Pavlov MY, Lovmar M, Ehrenberg M (2006) How initiation factors maximize the accuracy of tRNA selection in initiation of bacterial protein synthesis. *Mol Cell* 23(2):183–193.
6. Fortier PL, Schmitter JM, Garcia C, Dardel F (1994) The N-terminal half of initiation factor IF3 is folded as a stable independent domain. *Biochimie* 76(5):376–383.
7. Garcia C, Fortier PL, Blanquet S, Lallemand JY, Dardel F (1995) Solution structure of the ribosome-binding domain of E. coli translation initiation factor IF3. Homology with the U1A protein of the eukaryotic spliceosome. *J Mol Biol* 254(2):247–259.
8. Dallas A, Noller HF (2001) Interaction of translation initiation factor 3 with the 30S ribosomal subunit. *Mol Cell* 8(4):855–864.
9. Wang J, Caban K, Gonzalez RL, Jr (2015) Ribosomal initiation complex-driven changes in the stability and dynamics of initiation factor 2 regulate the fidelity of translation initiation. *J Mol Biol* 427(9):1819–1834.
10. Antoun A, Pavlov MY, Lovmar M, Ehrenberg M (2006) How initiation factors tune the rate of initiation of protein synthesis in bacteria. *EMBO J* 25(11):2539–2550.
11. Allen GS, Zavialov A, Gursky R, Ehrenberg M, Frank J (2005) The cryo-EM structure of a translation initiation complex from Escherichia coli. *Cell* 121(5):703–712.
12. Myasnikov AG, et al. (2005) Conformational transition of initiation factor 2 from the GTP- to GDP-bound state visualized on the ribosome. *Nat Struct Mol Biol* 12(12):1145–1149.
13. Tomsic J, et al. (2000) Late events of translation initiation in bacteria: A kinetic analysis. *EMBO J* 19(9):2127–2136.
14. Grigoriadou C, Marzi S, Kirillov S, Gualerzi CO, Cooperman BS (2007) A quantitative kinetic scheme for 70 S translation initiation complex formation. *J Mol Biol* 373(3):562–572.
15. Grigoriadou C, Marzi S, Pan D, Gualerzi CO, Cooperman BS (2007) The translational fidelity function of IF3 during transition from the 30 S initiation complex to the 70 S initiation complex. *J Mol Biol* 373(3):551–561.
16. Milon P, Konevega AL, Gualerzi CO, Rodnina MV (2008) Kinetic checkpoint at a late step in translation initiation. *Mol Cell* 30(6):712–720.
17. La Teana A, Pon CL, Gualerzi CO (1993) Translation of mRNAs with degenerate initiation triplet AUU displays high initiation factor 2 dependence and is subject to initiation factor 3 repression. *Proc Natl Acad Sci USA* 90(9):4161–4165.
18. Elvekrog MM, Gonzalez RL, Jr (2013) Conformational selection of translation initiation factor 3 signals proper substrate selection. *Nat Struct Mol Biol* 20(5):628–633.
19. Yusupov MM, et al. (2001) Crystal structure of the ribosome at 5.5 A resolution. *Science* 292(5518):883–896.
20. Voorhees RM, Weixlbaumer A, Loakes D, Kelley AC, Ramakrishnan V (2009) Insights into substrate stabilization from snapshots of the peptidyl transferase center of the intact 70S ribosome. *Nat Struct Mol Biol* 16(5):528–533.
21. Ali IK, Lancaster L, Feinberg J, Joseph S, Noller HF (2006) Deletion of a conserved, central ribosomal intersubunit RNA bridge. *Mol Cell* 23(6):865–874.
22. Liu Q, Fredrick K (2013) Contribution of intersubunit bridges to the energy barrier of ribosomal translocation. *Nucleic Acids Res* 41(1):565–574.
23. Hennelly SP, et al. (2005) A time-resolved investigation of ribosomal subunit association. *J Mol Biol* 346(5):1243–1258.
24. Pavlov MY, Zorzet A, Andersson DI, Ehrenberg M (2011) Activation of initiation factor 2 by ligands and mutations for rapid docking of ribosomal subunits. *EMBO J* 30(2):289–301.
25. Qin D, Liu Q, Devaraj A, Fredrick K (2012) Role of helix 44 of 16S rRNA in the fidelity of translation initiation. *RNA* 18(3):485–495.
26. Petrelli D, et al. (2001) Translation initiation factor IF3: Two domains, five functions, one mechanism? *EMBO J* 20(16):4560–4569.
27. Zhou Z, et al. (2007) Genetically encoded short peptide tags for orthogonal protein labeling by Sfp and AcpS phosphopantetheinyl transferases. *ACS Chem Biol* 2(5):337–346.
28. Reinbolt J, Tritsch D, Wittmann-Liebold B (1979) The primary structure of ribosomal protein S7 from E. coli strains K and B. *Biochimie* 61(4):501–522.
29. Milon P, et al. (2007) Transient kinetics, fluorescence, and FRET in studies of initiation of translation in bacteria. *Methods Enzymol* 430:1–30.
30. Tsai A, et al. (2012) Heterogeneous pathways and timing of factor departure during translation initiation. *Nature* 487(7407):390–393.
31. Kipper K, Hetényi C, Sild S, Remme J, Liiv A (2009) Ribosomal intersubunit bridge B2a is involved in factor-dependent translation initiation and translational processivity. *J Mol Biol* 385(2):405–422.
32. Sussman JK, Simons EL, Simons RW (1996) Escherichia coli translation initiation factor 3 discriminates the initiation codon in vivo. *Mol Microbiol* 21(2):347–360.
33. Qin D, Fredrick K (2009) Control of translation initiation involves a factor-induced rearrangement of helix 44 of 16S ribosomal RNA. *Mol Microbiol* 71(5):1239–1249.
34. MacDougall DD, Gonzalez RL, Jr (2015) Translation initiation factor 3 regulates switching between different modes of ribosomal subunit joining. *J Mol Biol* 427(9):1801–1818.
35. Cannone JJ, et al. (2002) The comparative RNA web (CRW) site: An online database of comparative sequence and structure information for ribosomal, intron, and other RNAs. *BMC Bioinformatics* 3:2.
36. Youngman EM, Green R (2005) Affinity purification of in vivo-assembled ribosomes for in vitro biochemical analysis. *Methods* 36(3):305–312.
37. Qin D, Abdi NM, Fredrick K (2007) Characterization of 16S rRNA mutations that decrease the fidelity of translation initiation. *RNA* 13(12):2348–2355.
38. Shoji S, Dambacher CM, Shajani Z, Williamson JR, Schultz PG (2011) Systematic chromosomal deletion of bacterial ribosomal protein genes. *J Mol Biol* 413(4):751–761.
39. McClory SP, Devaraj A, Fredrick K (2014) Distinct functional classes of ram mutations in 16S rRNA. *RNA* 20(4):496–504.